

Exciton recombination dynamics in *a*-plane (Al,Ga)N/GaN quantum wells probed by picosecond photo and cathodoluminescence

P. Corfdir,^{1,a)} P. Lefebvre,^{1,2} L. Balet,¹ S. Sonderegger,¹ A. Dussaigne,¹ T. Zhu,¹ D. Martin,¹ J.-D. Ganière,¹ N. Grandjean,¹ and B. Deveaud-Plédran¹

¹Institut de Photonique et d'Electronique Quantiques, Ecole Polytechnique Fédérale de Lausanne (EPFL), 1015 Lausanne, Switzerland

²Groupe d'Etude des Semiconducteurs, CNRS, Université Montpellier II, 34095 Montpellier, France

(Received 2 December 2009; accepted 5 January 2010; published online 25 February 2010)

We present a combined low-temperature time-resolved cathodoluminescence and photoluminescence study of exciton recombination mechanisms in a 3.8 nm thick *a*-plane (Al,Ga)N/GaN quantum well (QW). We observe the luminescence from QW excitons and from excitons localized on basal stacking faults (BSFs) crossing the QW plane, forming quantum wires (QWRs) at the intersection. We show that the dynamics of QW excitons is dominated by their capture on QWRs, with characteristic decay times ranging from 50 to 350 ps, depending on whether the local density of BSFs is large or small. We therefore relate the multiexponential behavior generally observed by time-resolved photoluminescence in non-polar (Al,Ga)N/GaN QW to the spatial dependence of QW exciton dynamics on the local BSF density. QWR exciton decay time is independent of the local density in BSFs and its temperature evolution exhibits a zero-dimensional behavior below 60 K. We propose that QWR exciton localization along the wire axis is induced by well-width fluctuation, reproducing in a one-dimensional system the localization processes usually observed in QWs. © 2010 American Institute of Physics. [doi:10.1063/1.3305336]

The current interest in the growth of non-polar nitride based quantum wells (QWs) is motivated by the possibility of eliminating the polarization fields observed in structures grown along the [0001] direction.¹ As a result of quantum confined Stark effect (QCSE), such built-in electric fields indeed produce a redshift of the emission wavelength and a decrease in the overlap between the electron and hole wave functions,² with detrimental consequences on the internal quantum efficiency of nitride-based light-emitting devices.³

Optical characterizations of (Al,Ga)N/GaN QWs grown along the non-polar [1120] *a*-axis have already demonstrated the circumvention of QCSE, fulfilling the primary expectations put into these heterostructures.^{3,4} However, even with optimized growth processes, such as epitaxial lateral overgrowth (ELO), *a*-plane GaN still suffers from high densities of extended defects, namely, dislocations and basal stacking faults (BSFs). While the former are nonradiative recombination centers, the latter are optically active.⁵ These planar inclusions of cubic-like GaN in the wurtzite phase can be seen as type-II QWs, where electrons are weakly confined in the well and holes are essentially located in the barriers.⁶ The emission properties of *a*-plane GaN depend on the spatial distribution of those BSFs, which, when gathered into high-density bundles, inhibit the emission from the usual donor bound exciton.⁷ Concerning non-polar heterostructures, a BSF will intersect perpendicularly the *a*-plane QW and therefore will generate a quantum wire (QWR) at the intersection, since the BSF suppresses one degree of freedom for two-dimensional excitons confined in the QW. However, even if clear optical signatures of such QWR excitons have

already been reported,⁸ quantitative information about their recombination dynamics and capture efficiency by the BSFs is still missing.

In this paper, we carry out a low-temperature time-resolved cathodoluminescence (TR-CL) study of exciton dynamics as a function of the local density of BSFs in an *a*-plane (Al,Ga)N/GaN single QW. We first demonstrate through CL experiments the existence of regions nearly free of any BSF as well as of regions with bundles of BSFs, indicating that the BSF distribution in the QW plane reproduces well the one of the underlying *a*-plane GaN templates. We confirm the results obtained by Badcock *et al.*,⁸ who demonstrated that the intersection of BSFs with the QW leads to the formation of QWRs, and we then study the local relaxation-recombination dynamics of excitons in both QW and QWRs. We show, in particular, that the dynamics of QW excitons is dominated by their capture by the BSFs and therefore exhibits a strong position dependency, explaining the large range of values reported so far for radiative lifetimes of excitons in non-polar (Al,Ga)N/GaN QWs.^{3,4} We finally demonstrate that below 60 K, QWR excitons exhibit a zero-dimensional behavior, which we relate to their binding on localization centers such as QW-width fluctuations.

The (Al,Ga)N/GaN single QW was grown by molecular beam epitaxy on a 15 μm thick *a*-plane ELO-GaN template grown by hydride vapor phase epitaxy on *r*-plane sapphire, the ELO mask consisting of 10 μm wide SiO₂ stripes aligned along the *m*-axis separated by 5 μm openings. The 3.8 nm wide GaN QW was grown between two (Al,Ga)N barriers of 155 (bottom) and 40 nm (top), respectively, with aluminum content set to 13%, as checked by high-resolution transmission electron microscopy and energy dispersive x-ray spectroscopy. Our picosecond TR-CL setup is based on

^{a)}Electronic mail: pierre.corfdir@epfl.ch.

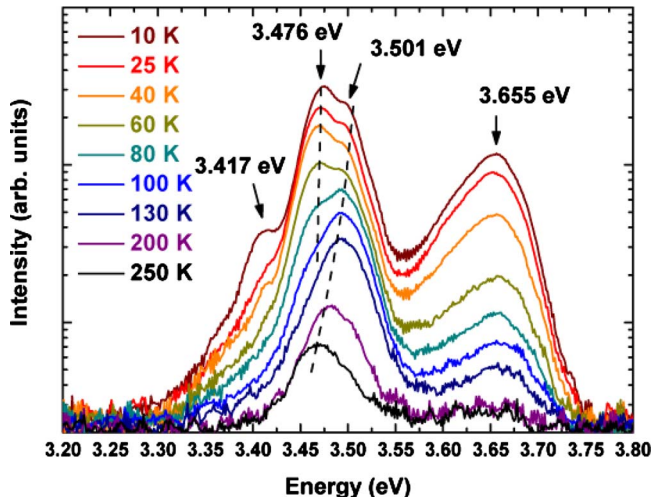


FIG. 1. (Color online) Time-integrated PL spectra of a 3.8 nm thick *a*-plane (Al,Ga)N/GaN QW taken at temperatures between 10 and 250 K. Dashed lines are guides for the eye.

a standard scanning electron microscope whose original electron gun was exchanged for a gold photocathode excited by the third harmonic of a pulsed Al₂O₃:Ti laser. We used an 8 kV acceleration voltage and focused the electron beam onto the sample surface with a 50 nm accuracy.⁹ The collected luminescence was dispersed by a 600 grooves per mm grating followed by a streak camera for time-resolved spectra. The overall time and spectral resolutions are 50 ps and 0.3 nm, respectively. The lower time resolution compared with our previous studies comes from the fact that the photocathode is now directly deposited on an optical fiber, which ensures a better spatial positioning of the electron source but also broadens temporally the excitation pulse. Time-integrated and time-resolved photoluminescence (PL) spectra were taken on a different setup by direct excitation with the third harmonic of a pulsed Al₂O₃:Ti laser (pulse width and repetition rate of 2 ps and 80.7 MHz, respectively) focused down to a 40 μm diameter spot on the sample surface.

Figure 1 displays the temperature (T) dependence of the time-integrated PL spectrum. The spectrum taken at 10 K exhibits two dominant emission lines at 3.501 and 3.476 eV, with full widths at half maximum of 30 and 26 meV, respectively (peaks were fitted by Gaussian curves). As shown in Fig. 1, we observe a relative increase in intensity with T of the higher energy line to the detriment of the 3.476 eV transition. This allows us to assign the latter to localized excitons within the QW that delocalize to the benefit of the higher-energy contribution, when T is increased. Quite generally, in (Al,Ga)N/GaN QWs, exciton localization is induced by well width fluctuations, leading to a single luminescence line at low T, and the thermally assisted delocalization produces a kink in the T-dependence of the PL peak energy, as excitons change from zero dimensional to bidimensional.¹⁰ In the case of a 3.8 nm thick QW, a one-monolayer increase in the well thickness results in a reduction in energy of $\sim 3\text{--}4$ meV (see Fig. 3 in Badcock *et al.*⁸). The splitting of 25 meV observed here is therefore too large to be caused by such a well-width fluctuation. Instead, as already observed and commented by Badcock *et al.*,⁸ this energy is more similar to the localiza-

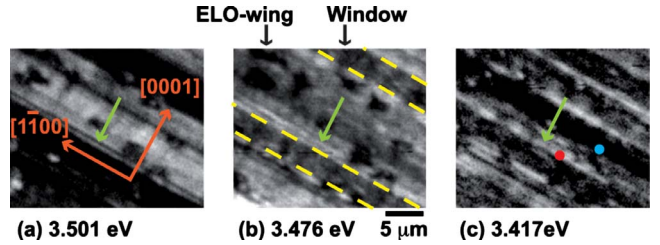


FIG. 2. (Color online) CL maps taken at 30 K at the emission energy of the (a) QW, of the (b) QWR, and of (c) BSFs in the GaN template. Arrows in (b) and (c) indicate the presence of bundles of BSFs, where the emission at 3.501 eV is inhibited. The dark blue and light red dots in (c) show where the excitation has been delivered to obtain the CL decays presented in Fig. 4.

tion energy of excitons on BSFs in bulk *a*-plane GaN (see below for further discussion), indicating that the 3.476 eV line is related to the intersection of BSFs with the QW. PL spectra also show weaker lines lying at 3.655 eV, corresponding to the (Al,Ga)N barriers and at 3.417 eV, which has been assigned to excitons bound to I₁-type BSFs in the GaN substrate.^{5,7,11}

In order to get further insight into the origin of the 3.476 eV line, we performed CL mappings of the near-band-edge luminescence (Fig. 2). When imaging the 3.476 eV CL [Fig. 2(b)], we observe long bright stripes perpendicular to the *c*-axis, anticorrelated with the QW emission at 3.501 eV [Fig. 2(a)] but in coincidence with the emission of BSF-bound excitons in bulk GaN at 3.417 eV [Fig. 2(c)]. Such spatial correlations and temperature dependent properties allow us to relate the 3.476 eV luminescence to QW excitons bound to BSFs, that is to say to QWR excitons, going along with the PL excitation measurements by Ref. 8. The clearer stripes in Fig. 2(b) therefore correspond to the intersection of the QW with BSFs gathered into high density bundles (linear density along [0001] about 10⁶ cm⁻¹),^{12,13} forming bundles of QWRs. Inversely, regions emitting mainly at the QW emission energy are associated with material where the BSF density is much smaller.

The time evolution of QW and QWR PL at 10 K is shown in Fig. 3(a). While the PL decay of QWR excitons exhibits a characteristic decay time of 430 \pm 10 ps, the QW emission shows a non-exponential behavior with fast and slow components of 50 \pm 5 and 350 \pm 10 ps, respectively. The PL of polar nitride-based QWs is expected to exhibit a non-exponential decay in specific cases: in ternary QWs such as (In,Ga)N/GaN due to localization effects induced by alloy disorder in the well,¹⁴ or even in binary QWs because of dynamic descreening of built-in electric fields.¹⁵ Non-exponential decays are also generally observed when analyzing temporally the PL of non-polar (Al,Ga)N/GaN QW.^{3,4} Although not yet discussed, this behavior is quite surprising as one would presume these polarization free (Al,Ga)N/GaN QWs to exhibit a luminescence with a monoexponential decay. However, one has to keep in mind that in usual PL experiments, the focus spot of the excitation laser beam has a diameter of several tens of micrometers. In our sample, where the periodicity of the ELO mask is 15 μm , the laser beam excites simultaneously the windows and both the +*c* and the -*c* ELO wings, i.e., morphologically different re-

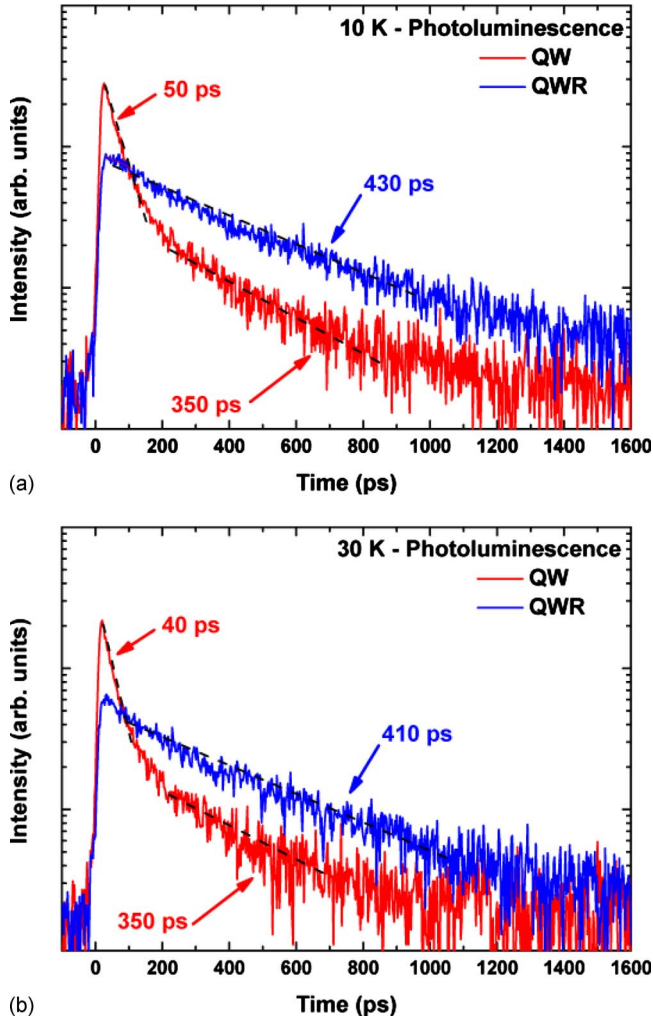


FIG. 3. (Color online) QW (light red) and QWR (dark blue) PL decays taken at 10 and 30 K [respectively (a) and (b)]. Black dashed lines and lifetimes are the results of mono-exponential fits.

gions of the sample where the linear density of BSFs along the [0001] exhibits local variations and ranges between 10^4 and 10^6 cm^{-1} .¹³ Therefore the observed PL certainly averages the signatures of excitons recombining in regions presenting a variety of BSF densities. To get a better insight into the role played by BSFs on QW exciton dynamics, we performed TR-CL experiments.

Indeed, TR-CL measured at T=30 K allowed us to probe the dynamics of QW excitons in different conditions of local BSF density. The first remarkable result is that the QWR CL shows a single-exponential decay with a characteristic decay time of 400 ± 20 ps (Fig. 4), independent of the local BSF density. The time constant agrees with TR-PL measurements at the same temperature [Fig. 3(b)]. On the other hand, the QW emission decay is now systematically found exponential, but the characteristic decay time depends drastically on where the excitation is delivered. When exciting directly on dense bundles of BSFs, the CL from QW excitons is weak, with a decay time that falls below the time resolution of our TR-CL setup (50 ps), indicating an efficient capture of these excitons by the QWRs [Fig. 4(b)]. When moving the excitation spot away from the bundles, i.e., to regions with lower densities in BSFs, the QW emission is

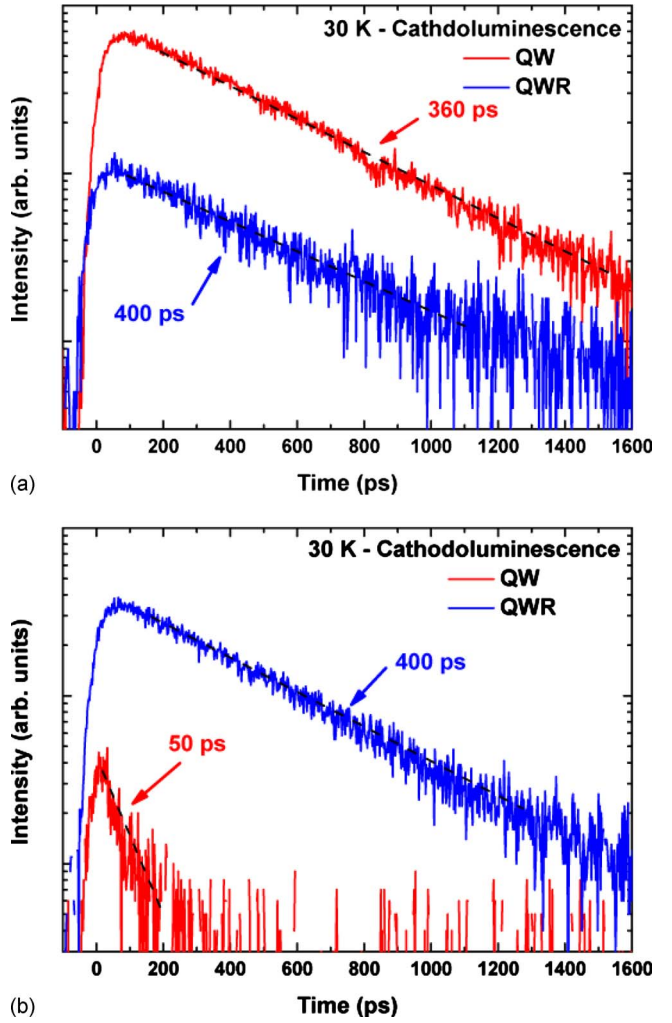


FIG. 4. (Color online) QW (light red) and QWR (dark blue) exciton CL decays taken at 30 K when exciting on low-density BSFs and on bundles of BSFs [respectively (a) and (b)]. Black dashed lines and lifetimes are the results of mono-exponential fits. The excitation spots for the CL decays shown in (a) and (b) correspond, respectively, to the dark blue and light red dots in Fig. 2(c).

enhanced and its decay time is about 360 ps [Fig. 4(a)]. TR-CL results confirm experimentally that the lifetime of QW excitons in non-polar (Al,Ga)N/GaN QWs reflects the local density in BSFs. This lifetime is limited by their capture dynamics onto BSFs, when the latter are in high densities. Elsewhere, when excitons are simply localized at well-width fluctuations, the transfer toward BSF-induced QWRs is slower and the observed 360 ps decay time, comparable to the decay time of excitons in narrow *c*-plane (Al,Ga)N/GaN QWs,¹⁶ reflects more certainly the radiative lifetime.

From these results, we clearly see that some precautions should be taken when analyzing the time-resolved PL of non-polar (Al,Ga)N/GaN QWs.

- (i) One should consider the slower component of the decay to account for the radiative recombination rate of excitons in the QW. At low temperature, these excitons are essentially localized at well-width fluctuations, and therefore one can be confident that the measured PL decay time is the radiative lifetime. The PL decay times presented by Ref. 4 consequently under-

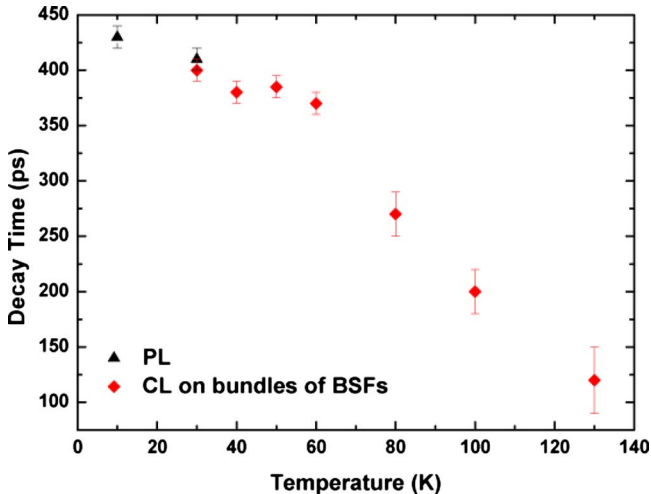


FIG. 5. (Color online) Decay time of the QWR emission with temperature obtained by time-resolved PL (triangles) and CL when the excitation is delivered on bundles of BSFs (diamonds).

estimate QW exciton radiative lifetimes.

- (ii) The faster component of the decay only represents the PL emission from excitons located in regions with high density bundles of BSFs. There, QW excitons experience a fast capture by the BSF-induced QWRs.
- (iii) The intensity ratio between the fast and slow decaying components of the QW PL gives a qualitative indication of the statistical distribution of BSFs between bundles and diluted BSFs within the region probed by the laser beam.

Now, let us note that as shown in Fig. 4(a), regions with low BSF densities do not exhibit the slow but efficient exciton capture rate (300 ps long) observed previously in bulk a -plane GaN.¹⁷ The diffusion of free excitons toward BSFs in bulk material has indeed been found to involve shallow donors via a kind of hopping process. Compared with the case of bulk GaN, the diffusion of excitons in the plane of the QW is indeed hindered by the presence of localization centers, such as well-width fluctuations¹⁰ or alloy fluctuation in the barriers.¹⁸ Whatever their origin, these potential fluctuations result in a reduced in-plane diffusion length of excitons: QWRs are therefore mostly populated either directly by the excitation pulse, or by the trapping of excitons through scattering processes occurring prior to their binding on usual QW potential fluctuation. In other words, we can assume that the effective diffusion length of excitons in the plane of the QW is more than 10 nm, as in the bundles (local BSF density about 10^6 cm^{-1}) they all reach a BSF before getting localized by well-width fluctuations. Similarly, this diffusion length is below 1 μm , since in the low BSF-density regions, where the average density in BSF is 10^4 cm^{-1} , excitons are in a large extent bound by localization centers induced by QW interface roughness before getting to BSFs.

When increasing T, the characteristic decay time of QWR CL keeps almost constant between 30 and 60 K and then decreases drastically for higher temperatures (Fig. 5). The evolution with T of QWR exciton decay rate therefore resembles that of a localized state: this rate remains constant

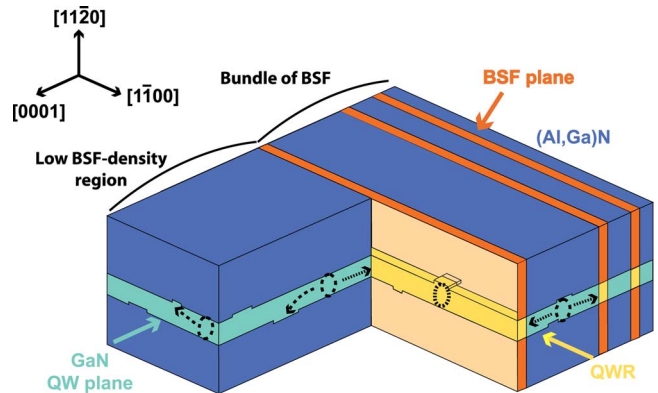


FIG. 6. (Color online) Schematic representation of exciton localization mechanisms in a -plane (Al,Ga)N/GaN QW. The intersection between the QW and the BSF planes forms a QWR. QW and QWR exciton wave functions (dashed and dotted black circles, respectively) are pinned on potential variation induced by QW-width fluctuations. In low BSF-density regions, there is competition between the diffusion of excitons toward BSFs (dotted black arrows) and the localization on well-width fluctuation (dashed black arrows), while in bundles of BSFs, excitons are trapped by the BSFs prior to their binding on well-width variation (dotted black arrows).

for $T < 60$ K, which is characteristic of zero-dimensional excitons. Since the width along [0001] of I₁-type BSF is fixed by nature at three monolayers,⁶ we suggest that the low temperature localization of excitons along the wires could be due to width fluctuations of the (Al,Ga)N/GaN QW, thus reproducing in a one dimensional system the localization scheme usually observed in (Al,Ga)N/GaN QWs (Fig. 6).¹⁰ In any case, the decay of QWR excitons at temperatures below 60 K is essentially radiative and we attribute the longer decay time of localized QWR excitons compared with that of localized QW excitons (400 and 360 ps, respectively) to the larger degree of localization of QWR excitons and consequently to the larger expansion of their wave function in reciprocal space.

For temperatures above 60 K, these zero-dimensional excitons become delocalized into the whole QWR and then can start reaching non-radiative centers, resulting in an increased effective decay rate of these excitons. For example, partial dislocations bounding the BSFs could be one cause of the quenching.¹² The situation is actually made complex by the fact that simultaneously, the increase in T allows the thermally activated escape of excitons from the QWR toward the QW. This induces the overall quenching of QWR luminescence to the benefit of QW emission, as observed in Fig. 1, so that it is difficult to ascertain the role of nonradiative defects.

In conclusion, we have performed TR-CL on a 3.8 nm wide a -plane (Al,Ga)N/GaN single QW. CL mappings and the evolution of the luminescence with temperature confirm that the intersection between BSFs and the QW leads to the formation of QWRs. We have shown that exciton dynamics in the QW depends drastically on the local density in BSFs and that the QW emission shows a decay time of 50 and 360 ps in high and low BSF density regions, respectively. The spatial dependence of QW exciton dynamics consequently explains the multi-exponential behavior generally observed by TR-PL experiments in non-polar (Al,Ga)N/GaN QWs. On

the contrary, the QWR luminescence decay time has been found independent of the local BSF density and we propose the localization of QWR excitons along the wire axis for temperatures below 60 K to be induced by QW-width fluctuations.

The authors acknowledge the *Attolight* Co. for the improvement of the TR-CL setup. We thank R. Rochat, N. Leiser, Y. Trolliet, H. J. Buehlmann, and D. Trolliet for technical assistance and the Swiss National Science Foundation for financing through Quantum Photonics NCCR and Project No. 119840.

- ¹F. Bernardini and V. Fiorentini, *Phys. Rev. B* **57**, R9427 (1998).
- ²P. Lefebvre, J. Allègre, B. Gil, H. Mathieu, N. Grandjean, M. Leroux, J. Massies, and P. Bigenwald, *Phys. Rev. B* **59**, 15363 (1999).
- ³P. Waltereit, O. Brandt, A. Trampert, H. T. Grahn, J. Menniger, M. Ramsteiner, M. Reiche, and K. H. Ploog, *Nature (London)* **406**, 865 (2000).
- ⁴N. Akopian, G. Bahir, D. Gershoni, M. D. Craven, J. S. Speck, and S. P. DenBaars, *Appl. Phys. Lett.* **86**, 202104 (2005).
- ⁵R. Liu, A. Bell, F. A. Ponce, C. Q. Chen, J. W. Yang, and M. A. Khan, *Appl. Phys. Lett.* **86**, 021908 (2005).
- ⁶C. Stampfl and C. G. Van de Walle, *Phys. Rev. B* **57**, R15052 (1998).
- ⁷P. Corfdir, P. Lefebvre, J. Levrat, A. Dussaigne, J. D. Ganière, D. Martin, J. Ristić, T. Zhu, N. Grandjean, and B. Deveaud-Plédran, *J. Appl. Phys.* **105**, 043102 (2009).

- ⁸T. J. Badcock, P. Dawson, M. J. Kappers, C. McAleese, J. L. Hollander, C. F. Johnston, D. V. Sridhara Rao, A. M. Sanchez, and C. J. Humphreys, *Appl. Phys. Lett.* **93**, 101901 (2008).
- ⁹M. Merano, S. Sonderegger, A. Crottini, S. Collin, P. Renucci, E. Pelucchi, A. Malko, M. H. Baier, E. Kapon, B. Deveaud, and J. D. Ganière, *Nature (London)* **438**, 479 (2005).
- ¹⁰M. Leroux, N. Grandjean, M. Latüg, J. Massies, B. Gil, P. Lefebvre, and P. Bigenwald, *Phys. Rev. B* **58**, R13371 (1998).
- ¹¹P. P. Paskov, R. Schifano, B. Monemar, T. Paskova, S. Figge, and D. Hommel, *J. Appl. Phys.* **98**, 093519 (2005).
- ¹²Z. H. Wu, A. M. Fischer, F. A. Ponce, B. Basteck, J. Christen, T. Wernicke, M. Weyers, and M. Kneissl, *Appl. Phys. Lett.* **92**, 171904 (2008).
- ¹³T. Gühne, Z. Bougrioua, P. Vennégùès, M. Leroux, and M. Albrecht, *J. Appl. Phys.* **101**, 113101 (2007).
- ¹⁴P. Lefebvre, A. Morel, M. Gallart, T. Talierco, J. Allègre, B. Gil, H. Mathieu, P. Damilano, N. Grandjean, and J. Massies, *Appl. Phys. Lett.* **78**, 1252 (2001).
- ¹⁵A. Reale, G. Massari, A. Di Carlo, P. Lugli, A. Vinattieri, D. Alderighi, M. Colocci, F. Semond, N. Grandjean, and J. Massies, *J. Appl. Phys.* **93**, 400 (2003).
- ¹⁶P. Lefebvre, J. Allègre, B. Gil, A. Kavokine, H. Mathieu, W. Kim, A. Salvador, A. Botchkarev, and H. Morkoç, *Phys. Rev. B* **57**, R9447 (1998).
- ¹⁷P. Corfdir, J. Ristić, P. Lefebvre, T. Zhu, D. Martin, A. Dussaigne, J.-D. Ganière, N. Grandjean, and B. Deveaud-Plédran, *Appl. Phys. Lett.* **94**, 201115 (2009).
- ¹⁸M. Gallart, A. Morel, T. Talierco, P. Lefebvre, B. Gil, J. Allègre, H. Mathieu, N. Grandjean, M. Leroux, and J. Massies, *Phys. Status Solidi A* **180**, 127 (2000).